Isotopic reversals with respect to maturity trends due to mixing of primary and secondary products in source rocks

Xinyu Xia [a,b,1], James Chen [a], Robert Braun [a], Yongchun Tang [b,*]

[a] GeoIsoChem Corporation, Covina, CA 91723, USA
[b] Power Environmental Energy Research Institute, Covina, CA 91722, USA

ABSTRACT

Carbon isotopic composition ($\delta^{13}C$) reversals with respect to maturity trends have been reported for ethane and propane in Barnett Shale gas in the Fort Worth Basin, U.S.A. This trend also exists in some conventional gas reservoirs, such as in the Ordos Basin, China and Appalachian Basin, U.S.A. Fractionation during mass transport is unlikely to be a significant mechanism, because its effect is minor under geological conditions, it would have caused more obvious reversal for methane than for ethane and propane, and mass transport can not account for the occurrence of the trend both inside and outside source rocks. This paper demonstrates that the reversal may result from mixing of indigenous primary gas (generated directly from kerogen) and secondary gas (generated from oil and condensate) within source rocks, and presents deconvolution results using end-members derived from a kinetic isotope fractionation model. The results, including the wetness and mixing ratio of primary and secondary gases, are consistent with geological conditions. Condensates may be the major precursor of the secondary gas in shale when the reversal occurs. A complete trend of $\delta^{13}C$ variations in methane and ethane with maturity is proposed that is based on the indigenous mixing mechanism.

© 2012 Elsevier B.V. All rights reserved.

1. Introduction

The recent accelerated exploration of shale gas provides an unprecedented opportunity to understand the geochemical processes in oil and gas source rocks. Detailed distributions and compositions of oil, gas and other organic matter in source rocks have been investigated by organic and gas isotopic geochemistry, especially the analysis of carbon isotopic compositions ($\delta^{13}C$) of alkanes, which are among the few geochemical indices of natural gas. Interestingly, abnormal trends in $\delta^{13}C$ values are revealed by the shale gas data (Zumberge et al., 2009, 2012).

Normal trends of alkane $\delta^{13}C$ values in natural gas are fundamentally determined by the kinetic process of natural gas generation from precursors (kerogen, bitumen, oil and condensates). Specifically, the trends are determined by a kinetic isotope effect (KIE) resulting from differences in energy required for cleavage of $^{12}C-^{12}C$ and $^{12}C-^{13}C$ bonds in the precursors (Tang et al., 2000). KIE brings about a more positive carbon isotopic composition in the hydrocarbon at higher maturity. KIE is more profound for smaller molecules due to the increasing relative differences of molecular weights between their isotopologues. Therefore, two normal trends are expected:

1) $\delta^{13}C$ values of each gaseous hydrocarbon component become more positive with increasing maturity (Stahl and Carey, 1975; Stahl et al., 1977; Schoell, 1983). The maturity of thermogenic gas may be expressed indirectly by increasing vitrinite reflectance (R_o), or directly by decreasing gas wetness (volume percentage of ethane through pentane hydrocarbons in natural gas).

2) $\delta^{13}C$ values are more positive with increasing carbon number from methane ($\delta^{13}C_1$), ethane ($\delta^{13}C_2$) to propane ($\delta^{13}C_3$) at identical maturity ($\delta^{13}C_1 < \delta^{13}C_2 < \delta^{13}C_3$).

While much of the conventional and shale gas geochemical data follows the above trends (for shale gas examples see Hill et al., 2007), reversed isotopic trends are common. $\delta^{13}C$ reversals with respect to carbon number ($\delta^{13}C_1 > \delta^{13}C_2$ and/or $\delta^{13}C_2 > \delta^{13}C_3$) have been found in some shale gas plays in the U.S. (Zumberge et al., 2012). This trend is not unique in shale gas; it has also been found in conventional reservoirs in the U.S. (Jenden and Drazan, 1993; Burruss and Laughrey, 2010), China (Xia et al. 1999, Dai et al., 2004), and Canada (Tilley et al., 2011). The other reversed trend, $\delta^{13}C$ with respect to maturity, is remarkable for ethane and propane in some shale gas plays (Zumberge et al., 2009, 2012) and has drawn much attention due to its relation to gas productivity (Brown, 2010). The $\delta^{13}C_2$ reversal with respect to maturity trends was also found in some conventional reservoirs, such as in the Ordos Basin in China (Xia et al., 1999).

Various mechanisms have been proposed to explain the two types of reversal. For $\delta^{13}C$ reversals with respect to carbon number, mixing of natural gas of different origins is regarded as the main mechanism (Jenden and Drazan, 1993; Dai et al., 2004). This mechanism seems favorable in basins having multiple source rocks containing different

kerogens or having different maturities. For example, in the Ordos Basin, the $\delta^{13}C$ reversal with respect to carbon number has been attributed to mixing of gases from humic kerogen (more positive $\delta^{13}C$) and sapropelic kerogen (more negative $\delta^{13}C$). However, the deconvoluting results based on constant $\delta^{13}C$ values for the two end-members appears to be inconsistent with the relation between $\delta^{13}C_2$ and wetness (Xia et al., 1999, Fig. 2).

After the $\delta^{13}C_2$ reversal with respect to wetness in shale gas was discovered, a preliminary interpretation was proposed that involved mechanisms related to both generation and mass transport (Zumberge et al., 2012). A quantitative interpretation of these observations is still required to advance knowledge of the geochemical processes in source rocks and to improve natural gas resource evaluation. The main purpose of this paper is to provide a quantitative evaluation of the different mechanisms for the reversed isotope trends in shale gas and in conventional gas reservoirs, especially the mechanism of mixing gases generated from different processes. The quantitative deconvolution calculation will provide a critical evaluation of the mechanism and will improve understanding of gas generation.

2. Geological settings and geochemical data

2.1. Geological settings

Natural gas geochemical data from three basins were investigated. The $\delta^{13}C_2$ reversal was found in each basin, including the Fort Worth and Appalachian basins in the U.S. and the Ordos Basin in China. The molecular and carbon isotopic compositions of natural gas from the three basins were mainly reported by Zumberge et al. (2012), Dai et al. (2005), and Burruss and Laughrey (2010). The geological conditions of hydrocarbon generation were investigated in previous studies (Dai et al., 2005; Hill et al., 2007; Burruss and Laughrey, 2010 and references therein). Brief descriptions of the source and reservoir rocks are listed in Table 1.

These conventional and the unconventional reservoirs share several similar geological characteristics. The petroleum occurs in stratigraphic traps and the deformation of reservoir rocks is relatively gentle (though carbonates in the basins may be fractured). Major faults did not develop during the recent uplift movements after the reservoir formed. Finally, the reservoirs are vertically close to the source rocks, resulting in short migration distances.

2.2. Isotopic reversal with respect to wetness in published field data

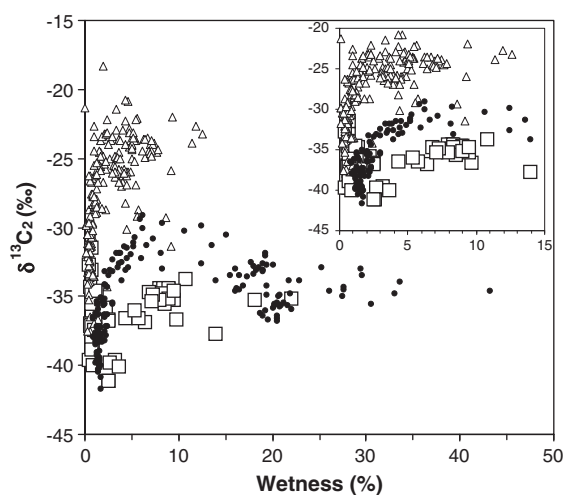The isotopic reversal with respect to maturity is obvious on the plot of $\delta^{13}C_2$ versus gas wetness (Zumberge et al., 2012, Fig. 2; Xia et al., 1999, Fig. 2; Burruss and Laughrey, 2010, Fig. 10). Fig. 1 summarizes data from the three basins. Note that wetness is a reliable parameter for source rock maturity. If the gas reservoir conditions and the source rock organic types are similar: wetness decreases monotonically with maturity at $R_o > 0.8\%$ (for coal-formed gas see Rice, 1993; for shale gas see Hill et al., 2007).

In Fig. 1, at high wetness (low maturity), $\delta^{13}C_2$ values of gas from the Fort Worth Basin become more positive with decreasing wetness, which is the normal trend during gas generation. This variation is not as obvious in other two basins. When gas wetness drops to a critical point, the reversed trend is observed, not only for shale gas from the Fort Worth Basin (critical wetness of ~4%), but also for the conventional gas reservoirs in the Ordos Basin(critical wetness of ~2%) and in the Appalachian Basin (with critical wetness ~10%). The drop of $\delta^{13}C_2$ values is over 10‰ for the Ordos and Fort Worth basins. The occurrence of this reversal is independent of organic type in source rocks and of gas isotope composition ($\delta^{13}C_2$ for the Ordos Basin are the most positive and while values for the Appalachian Basin are the most negative). Interestingly, when wetness is very low (< 1 vol%), the gas from the Appalachian Basin regains the normal trend of $\delta^{13}C_2$ with respect to wetness (based on 20 samples in Fig. 1).

Similar normal and reversal trends are found for $\delta^{13}C_3$ as well (Fig. 2A); but the $\delta^{13}C_1$ values seem to increase monotonically with decreasing wetness, with some vague reversed and back-to-normal trends at wetness<5 % (Fig. 2B). Because the reversal is stronger for $\delta^{13}C_2$ than for $\delta^{13}C_1$, when the maturity is high enough, there could be $\delta^{13}C_2 < \delta^{13}C_1$. Thus, the $\delta^{13}C$ reversals with respect to carbon number and maturity trend may result from the same mechanism.

Similar to the above isotope trends, an initial increase followed by a decrease of isobutane to n-butane ratio (iC_4/nC_4) with respect to maturity trend was also revealed (Fig. 3). The reverse may reflect faster generation of n-butane than isobutane, and/or faster decomposition of isobutane than n-butane at high maturity. The latter seems more probable, because isobutane is kinetically less stable than n-butane (the tertiary C–H bond in isobutane is more active due to stabilized tertiary radicals). Thus, the iC_4/nC_4 and $\delta^{13}C_2$ reversals may not result from the same process.

Other special trends include increased CO_2 concentrations and reversal $\delta^{13}C$ of CO_2 at higher maturity (Fig. 4 in Zumberge et al., 2012), and a methane hydrogen isotope (δ^2H_1) reversal with respect to maturity trend

Table 1
Source rocks and reservoirs of gas fields having isotopic reversals with respect to maturity.

	Fort Worth Basin[1]	Ordos Basin[2]	Appalachian Basin[3]
Reservoir	Mississippian Barnett Shale	C–P terrigeneous sand; C limestone; O weathered crust	O–S tight sand, fractured carbonate and shale
Source rock	Mississippian Barnett Shale	C–P coal measures	O Utica Shale
TOC (wt %)	4.5	1–60 (coal)	1.8
Organic type	II	III	II
R_o (%)	0.8–>2.1	1.2–3 bottom Carboniferous	1–4
Thickness (m)	30 – 200	30–120	20–300

1 — Zumberge et al. (2012); 2 — Dai et al. (2005); 3 — Burruss and Ryder (2003), Burruss and Laughrey (2010), Repetski et al. (2008); C=Carboniferous; P=Permian; O=Ordovician; S=Silurian.

Fig. 1. Wetness-dependent variation of $\delta^{13}C_2$ (ethane) in natural gas from the Ordos Basin (triangles, Dai et al., 2005; Xia, 2000; Hu et al., 2008), the Fort Worth Basin (dots, Zumberge et al., 2012), and the Appalachian Basin (squares, Burruss and Laughrey, 2010). Wetness is defined as the volume fraction of C_{2+} gaseous hydrocarbon in total gaseous hydrocarbon. Inset shows a selected portion of the full data.
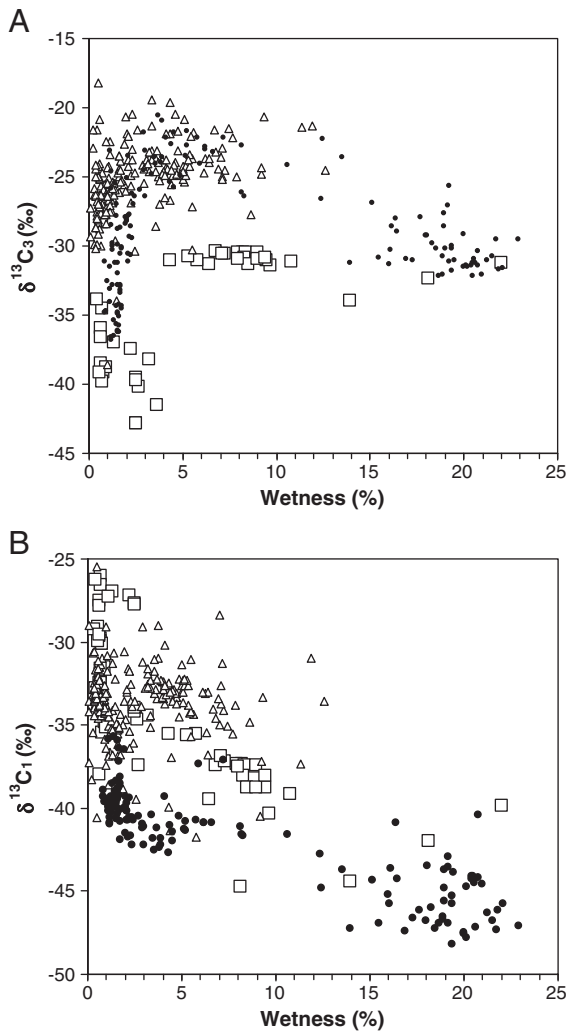
Fig. 2. Wetness-dependent variation of $\delta^{13}C_3$ (propane, A) and of $\delta^{13}C_1$ (methane, B) in natural gas from the Ordos Basin (triangles, Dai et al., 2005; Xia, 2000; Hu et al., 2008), the Fort Worth Basin (dots, Zumberge et al., 2012), and the Appalachian Basin (squares, Burruss and Laughrey, 2010).

in the Appalachian Basin (Fig. 5 in Burruss and Laughrey, 2010). Their relation to the $\delta^{13}C_2$ and $\delta^{13}C_3$ reversals discussed in the present paper requires further research.

3. The mixing model

3.1. Indigenous generation and mixing as a mechanism for isotopic reversal

Gas isotope fractionation may result from both chemical processes (hydrocarbon generation and cracking) and mass transport (adsorption/desorption and diffusion). Because organic-rich shale is a good hydrocarbon adsorbent, and because diffusion plays an important role in gas flow through the micropore system in shale (Passey et al., 2010), mass transport needs to be considered as a cause for the $\delta^{13}C_2$ reversal in shale gas. However, the reversal also appears in conventional gas reservoirs (composed of organic-poor sandstone and carbonates) in the Ordos Basin. Therefore, fractionation due to gas moving through shale is unlikely to be the main reason for the reversal, regardless of whether the fractionation is caused by adsorption/desorption or diffusion. Our recent work indicates that mass transport (adsorption/desorption and diffusion) causes very little isotopic fractionation of methane during expulsion or gas production from shale (<3‰, Xia and Tang, 2012); the fractionation would be even smaller for ethane and propane due the decreased relative molecular masses. Thus, mass transport seems unlikely to have caused the $\delta^{13}C$ reversal of up to 10‰. We conclude that these abnormal trends are caused by indigenous mechanisms in the source rocks and remain after migration to the conventional reservoirs.

Indigenous mechanisms of gas generation include processes other than kerogen-cracking (primary generation). Most likely these processes result in the conversion of the intermediate products from kerogen (oil, condensates, and/or heavy gases) to light gases. In this secondary process, isotope fractionation is stronger and the products more enriched in ^{12}C. As discussed for Fig. 3, isobutane becomes unstable at high maturity, indicating that some branched compounds in condensates may start to crack. On the other hand, $\delta^{13}C_2$ and $\delta^{13}C_3$ values become more negative after the wetness drops to the critical wetness points (Figs. 1 and 2A), indicating that the straight-chain alkanes are still stable at high maturity.

Isotopic reversal caused by mixing of primary and secondary generated gas can be explained using the scheme shown in Fig. 4. Fractionation during primary generation results in more negative $\delta^{13}C$ values of oil, condensate and gas than that of the kerogen. Fractionation during secondary generation is much stronger (The activation energy for secondary generation is higher, thus its kinetic isotope fractionation effect is stronger, see Fig. 4 of Tang et al., 2000), rendering a much more negative $\delta^{13}C$ value of secondary generation gas than oil and condensates. Meanwhile, oil and condensate conversion, through the cleavage of carbon chains, produces much larger amount
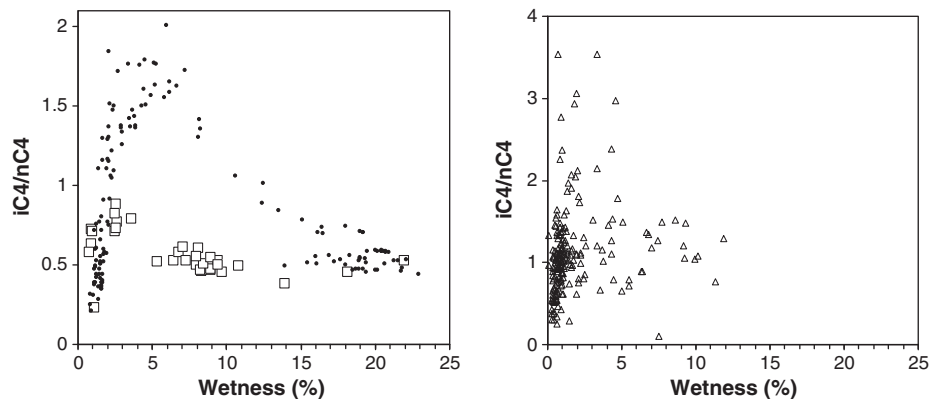
Fig. 3. Isobutane to *n*-butane ratio versus gas wetness in the Fort Worth Basin (dots, Zumberge et al., 2012), Appalachian Basin (squares, Burruss and Laughrey, 2010), and Ordos Basin (triangles, Dai et al., 2005; Xia, 2000; Hu et al., 2008).

of ethane and propane than does the demethylation of high maturity kerogen. Hence, the secondary gas is "wetter" and has more negative $\delta^{13}C$ values than primary gas at high maturity. As a result, in a mixture of primary and secondary gas at high maturity, methane is dominantly contributed from the former and ethane is dominantly from the latter; isotopic reversal with respect to carbon number will occur. Meanwhile, ethane and propane from secondary generation increases with maturity, bringing about a $\delta^{13}C_2$ reversal with respect to maturity trend.

3.2. Deconvoluting model and parameters

The mechanism of Fig. 4 has definite solutions by deconvolution, provided the values of wetness, $\delta^{13}C_1$ and $\delta^{13}C_2$ of the mixed gas, and the values of $\delta^{13}C_1$ and $\delta^{13}C_2$ of the end-members are known. Let us assume the molar ratio between primary and secondary gases is $1 : x$. For conciseness, only methane and ethane are taken into account. If the wetness values of the two end-members are w_k and w_o, respectively, then we have the following equations that consider the mass balance of wetness, ethane, and methane:

$$\begin{cases} (1+x)w_m = w_k + xw_o \\ xw_o = r_{C_2}w_k \\ x(1-w_o) = r_{C_1}(1-w_k) \end{cases} \tag{1}$$

Here w_m is wetness of the mixed gas; r_{C1} is the ratio of methane from the secondary gas ot that of the primary gas; r_{C2} is the ratio of ethane from the secondary gas to that of the primary gas. The values of r_{C1} and r_{C2} are known from mass balance of the isotopologues:

$$\begin{cases} r_{C_1} = \dfrac{\delta_{C_1,m} - \delta_{C_1,k}}{\delta_{C_1,o} - \delta_{C_1,m}} \\ r_{C_2} = \dfrac{\delta_{C_2,m} - \delta_{C_2,k}}{\delta_{C_2,o} - \delta_{C_2,m}} \end{cases} \tag{2}$$

where $\delta_{C1,k}$, $\delta_{C1,o}$, and $\delta_{C1,m}$ refer to $\delta^{13}C_1$ of the primary gas, secondary gas, and mixed gas, respectively; $\delta_{C2,k}$, $\delta_{C2,o}$, and $\delta_{C2,m}$ refer to $\delta^{13}C_2$ of the primary gas, secondary gas, and mixed gas, respectively. The only unknown parameters in equation group (1) are x, w_k and w_o as follows:

$$\begin{cases} x = \dfrac{r_{C_1}\left(1 + r_{C_2}\right) - w_m\left(r_{C_1} - r_{C_2}\right)}{1 + r_{C_2} + w_m\left(r_{C_1} - r_{C_2}\right)} \\[2ex] w_k = \dfrac{w_m\left(1 + r_{C_1}\right)}{1 + r_{C_2} + w_m\left(r_{C_1} - r_{C_2}\right)} \\[2ex] w_o = \dfrac{w_m r_{C_2}\left(1 + r_{C_1}\right)}{r_{C_1}\left(1 + r_{C_2}\right) - w_m\left(r_{C_1} - r_{C_2}\right)} \end{cases} \tag{3}$$

If the mixing mechanism is a reliable interpretation for isotopic reversals, then the deconvolution calculation should give reasonable geochemical solutions for the two end-members and their mixing ratios. To conduct the deconvolution, the first step is to determine the maturity-dependent $\delta^{13}C$ values for the primary and secondary gases ($\delta_{C1,k}$, $\delta_{C1,o}$, $\delta_{C2,k}$, and $\delta_{C2,o}$) for each of the three basins. The values may be derived based on the kinetic isotope fractionation (KIE) model described by Tang et al. (2000). In this model, gas carbon isotopic composition is determined by the $\delta^{13}C$ of its precursor, differences between the kinetic factors (activation energies and frequency factors) to break a $^{12}C - ^{12}C$ bond and a $^{13}C - ^{12}C$ bond in the precursors, and the generation/accumulation history. The kinetic parameters can be derived by calibrating with isobaric pyrolysis results of representative precursors. Theoretical derivation based on laboratorial experimental data is the only approach to obtain the isotopic composition of the secondary gas end-member, because in reality it is quite improbable
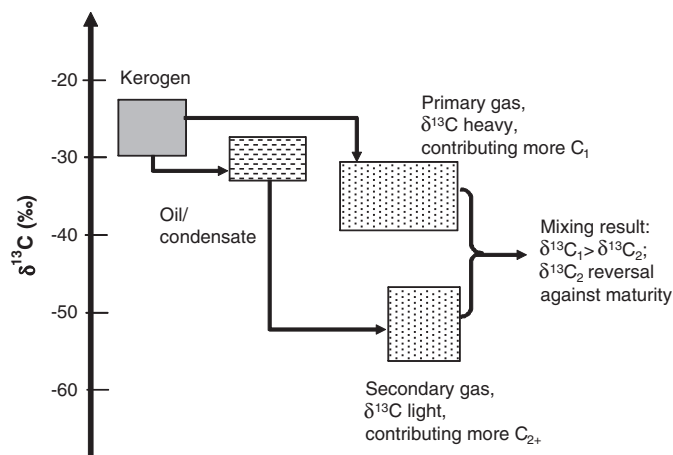

Fig. 4. Scheme showing $\delta^{13}C$ reversal due to mixing of primary and secondary gas.

that a gas reservoir is filled merely with secondary gas. Thus, the values for this end-member cannot be obtained from field data.

To derive the maturity-dependent $\delta^{13}C$ values for secondary gas, we calibrated the kinetic model using an oil sample generated from Ordovician marine shale in the Tarim Basin, China (data from Tian et al., 2010). The Type II organic matter in the source rock is similar to that of the Ordovician Utica Shale of the Appalachian Basin and the Barnett Shale in the Fort Worth Basin. Moreover, the $\delta^{13}C$ value of the Tarim Basin oil is $-32.1‰$, which is similar to the value of oil generated from Barnett Shale at low maturity ($-32‰$, Hill et al., 2007). The $\delta^{13}C$ values of oil generated from the Utica Shale are -30.2 to $-29.5‰$ (Burruss and Ryder, 2003), about 2 ‰ more positive than the Tarim Basin oil.

Similarly, we use the pyrolysis data reported by Tian et al. (2010) for a mature Ordovician marine kerogen (equivalent $R_o = 1.1\%$) to calibrate the kinetic model, in order to derive $\delta_{C1,k}$ and $\delta_{C2,k}$ for the gases from marine source rocks in the Fort Worth and Appalachian basins. Compared with pyrolysis of immature kerogen, pyrolysis of mature kerogen results in high-maturity gas generation similar to that generated under natural conditions. Calibrations were performed by means of GeoIsoChem Isotopes® and Kinetics05® software; the calibrated parameters are listed in Table 2.

Before projecting the $\delta^{13}C$ values to geological conditions, the accumulation extent needs to be taken into account. If all gas generated at different maturity stages is trapped in a single reservoir ("cumulative" conditions), then the $\delta^{13}C$ values of the gases will be more negative than those in a reservoir that trapped only the high-maturity gas ("instantaneous" conditions) (Tang et al., 2000). For primary gas we applied the instantaneous results, the time interval corresponds with an R_o interval of 0.4%. For secondary gas we applied the cumulative results. This assumption is reasonable considering a typical generation history: secondary gas generation occurs later than primary generation, so secondary gas is more likely to be retained in the source rock or in close-to-source reservoirs, while primary gas is more likely to be flushed away.

The above models were applied directly to derive the end-members for the Fort Worth and Appalachian basins. The extension to geological conditions was performed using GeoIsoChem GOR-Isotopes® software. Condensates generated from Permo-Carboniferous limestone in the Ordos Basin is $-26‰$ (Zhang and Li, 2001), which is remarkably more positive ($+6‰$) than the Tarim Basin Ordovician oil. For this reason, we shifted the $\delta^{13}C$ values of the Fort Worth and Appalachian Basin products by $+6‰$. For primary gas in the Ordos Basin, we applied the empirical R_o-$\delta^{13}C$ relations for coal-related gas in China summarized by Dai and Qi (1989).

$\delta^{13}C$ values of the end-members as functions of R_o are presented in Fig. 5, along with the natural gas isotope data of the three basins. The

corresponding R_o values of gas samples from the Fort Worth Basin were calculated approximately from the following equation, which is based on data from Zumberge et al. (2009, 2011) and Hill et al. (2007):

$$R_o = -0.33 \ln(w_m) + 2.2 \tag{4}$$

R_o values for the gas samples from the Ordos Basin were calculated using the following equation derived from data in Dai et al. (2005) and Xia et al. (1999):

$$R_o = -0.27 \ln(w_m) + 1.9 \tag{5}$$

R_o values for the gas samples from the Appalachian Basin were calculated using the following equation, based on data from Burruss and Laughrey (2010) and Repetski et al. (2008):

$$R_o = -0.74 \ln(w_m) + 3.3 \tag{6}$$

Fig. 5 indicates qualitatively that $\delta^{13}C_1$ and $\delta^{13}C_2$ for each end-member increase monotonically with R_o; the values of field data lie mainly between the curves of the end-member pairs. At R_o values between 1.5% and 2.0%, the $\delta^{13}C_2$ values of field data shift away from the curve of primary gas toward the curve of secondary gas. Although there is no obvious reversal for $\delta^{13}C_1$, it still deviates from the curve of
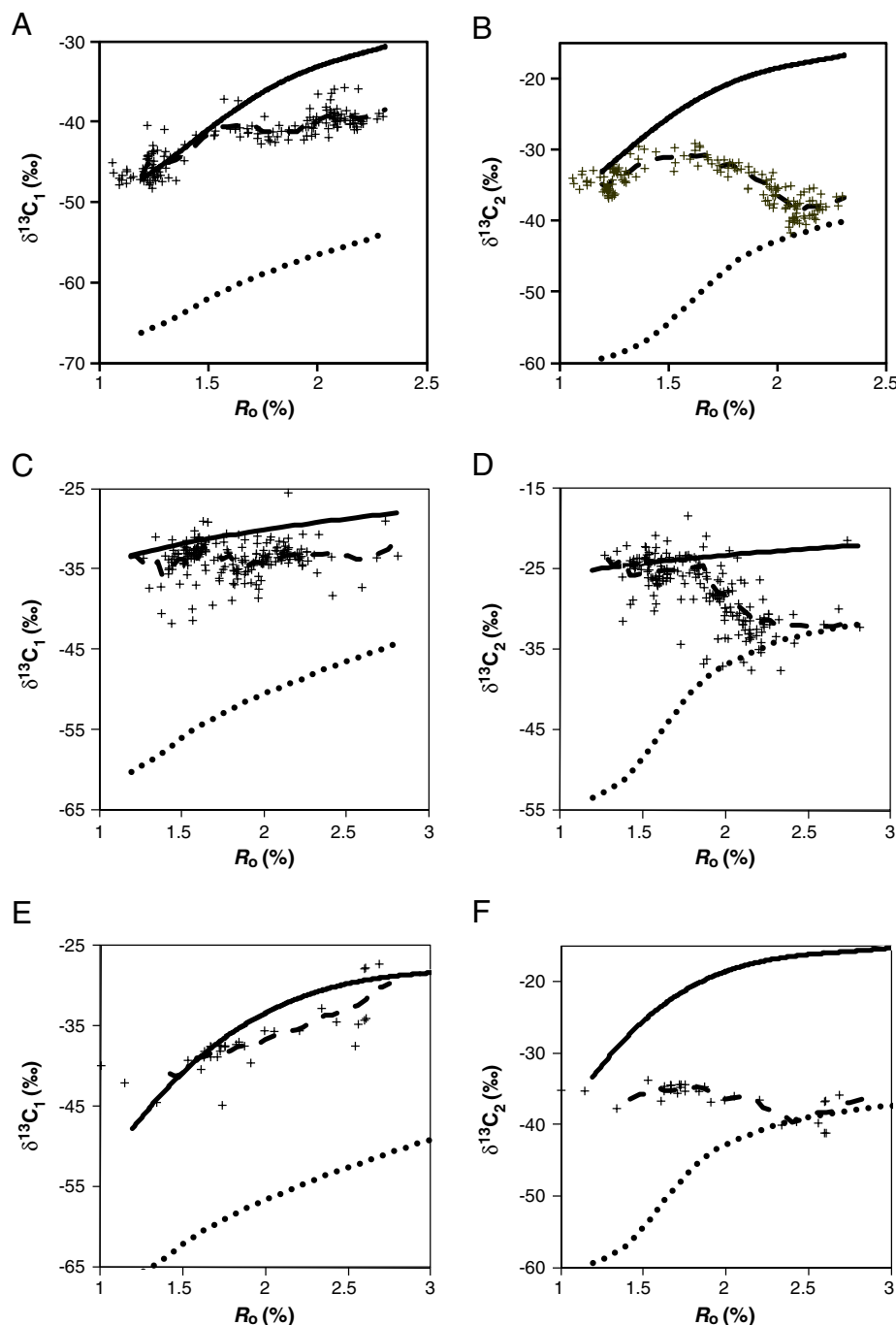
Fig. 5. $\delta^{13}C$ of methane (A, C, E) and ethane (B, D, F) in the gas end-members from primary generation (solid lines) and secondary generation (dotted lines), with field data from the Fort Worth Basin (A, B), the Ordos Basin (C, D), and the Appalachian Basin (E, F; data for calibrated Ro > 3% omitted). Dashed lines: moving average of the field data.

Table 2
Kinetic parameters for isotope fractionation during primary and secondary generation of methane and ethane.

Parameters	Primary generation		Secondary generation	
	Methane	Ethane	Methane	Ethane
A	1.02	1.02	1.02	1.02
E_0 (kcal /mol)	52.0	51.5	56.7	54.5
β_L (cal/mol)	0	11	0	0
β_H (cal/mol)	70	70	70	60
σ (kcal/mol)	2.44	2.34	6.56	11.2
γ (‰)	−34.5	−28.3	−40.9	−35.5

Note: α: ratio between frequency factors for ^{12}C–^{12}C and ^{13}C–^{12}C cleavages; E_0: central value of a Gaussian distribution of activation energy differences between ^{12}C–^{12}C and ^{12}C–^{13}C cleavages; β_L and β_H: the minimum and maximum values of activation energy difference between ^{12}C–^{12}C and ^{13}C-^{12}C, respectively; σ: the variance of a cumulative Gaussian function to describe the activation energy difference between ^{12}C–^{12}C and ^{13}C–^{12}C; γ: $\delta^{13}C$ of intermediate species at key fractionation step (Tang et al., 2000).

primary gas, indicating that methane from secondary generation is being contributed to the total methane. At lower maturity ($R_o < \sim 1.5\%$), almost all methane and ethane is from primary gas; while at higher maturity ($R_o > \sim 2.0\%$), almost all ethane is from secondary gas. The results are consistent with the model shown in Fig. 4.

3.3. Deconvoluting results

Fig. 5 along with Eqs. (4)–(6) provides the parameters required to solve Eq. (3) for each R_o value. The solutions, including the mixing ratio and wetness of primary and secondary gases at different maturity, are shown in Fig. 6. Fig. 6 illustrates that the wetness of primary gas decreases with respect to maturity trend. Regardless of how the wetness of secondary gas varies, it exceeds the wetness of primary gas in the high maturity range.

In the computations above, we considered how $\delta^{13}C_1$ and $\delta^{13}C_2$ vary with maturity and rationalized that isotopic reversal between methane and ethane, i.e., $\delta^{13}C_1 > \delta^{13}C_2$, can take place due to a mixing mechanism. To investigate a fuller isotopic reversal over a longer carbon number series, i.e., $\delta^{13}C_1 > \delta^{13}C_2 > \delta^{13}C_3$, which phenomenon has been observed in Appalachian and other basins (Burruss and Laughrey, 2010), propane needs to be incorporated into the computations. Using methods similar to those described in the context of Eqs. (1)–(3), we can deconvolute contributions from propane together with methane and ethane, from both primary and secondary gases. As an example, Table 3 presents a case of full isotopic reversal trend that has been deconvoluted, with all resulting fractional contributions falling within reasonable ranges.

4. Discussion

4.1. Viability of the mechanism

To check the viability of this mixing mechanism, we need to consider whether the solutions are in reasonable ranges. All solved wetness values (<30%) are in the normal range for field gases. The contribution of secondary gas is over 20% for the cases in the Fort Worth and Appalachian Basins at $R_o > \sim 2\%$; their precursor should be mainly condensate instead of oil, because at such high maturity most oil would have already been expelled from the source rocks. So the question is, whether there is enough residual condensate in the source rock to account for these observations. Recent unconventional exploration indicates that condensates dominate the hydrocarbon fluids in much of the Eagle Ford Shale in the U.S. (Mullen and Lowry, 2010), and exist in the Barnett Shale as well (Zumberge et al., 2009). Therefore, it is possible that condensates act as the precursor of secondary gas in shale. As for the Ordos Basin, the secondary gas contributes up to 30% of the total gas in some cases. The source for this secondary gas may include wax and condensates retained in Carboniferous coal source rock due to its strong
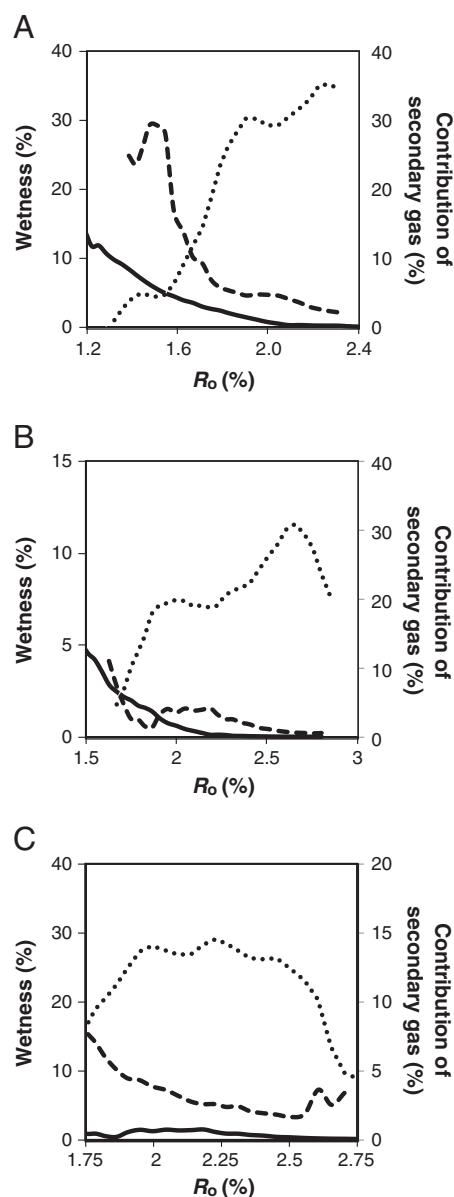
Fig. 6. Wetness of primary gas (solid lines) and secondary gas (dashed lines) along with contribution of secondary gas (dotted lines) as solved from Eq. (3) with parameters shown in Fig. 5 for the natural gases from the Fort Worth Basin (A), the Ordos Basin (B), and the Appalachian Basin (C).

Table 3
Deconvolution of a gas sample with full reversal.

Parameters	Mixture[a]	Primary gas	Secondary gas
Isotopic composition ($\delta^{13}C$, ‰)			
CH_4	−33.97	−33.67 [b] 11	−57.4 [b]
C_2H_6	−41.15	−19 [b] 11	−44.4 [b]
C_3H_8	−42.81	−16 [b] 11	−42.9 [b]
Molecular composition (mol %)			
CH_4	97.5	99.7 [c] 11	36.4 [c]
C_2H_6	2.31	0.31 [c] 1	59.6 [c]
C_3H_8	0.13	0.00047 [c]	4.0 [c]
Mixing ratio		96.62% [c]	3.38% [c]

Note: a: from Burruss and Laughrey (2010), the last sample in Table 1; b: assumed end-member values; c: deconvolution results.

adsorption capacity (Rice et al., 1989). Based on the above, the amounts of precursors for the secondary generation in source rocks appear to be sufficient and consistent for the model.

The results in Fig. 6 should be regarded as semi-quantitative. The uncertainties in the above calculation owe mainly to the following factors: 1) heterogeneity of organic matter distribution and oil/gas migration, which is reflected by the scattered $\delta^{13}C$ data with respect to wetness and R_o, and 2) uncertainty of the relation between wetness and R_o. When $\delta^{13}C$ values of field data are close to the end-member curves, the results are very sensitive to errors. Nevertheless, the calculation successfully demonstrates that reversed isotopic trends caused by mixing are possible.

It should be noticed that the mechanism of condensate conversion to gas is not fully understood and not discussed in this paper. The reversed trend of hydrogen isotopic composition with depth in the Appalachian Basin (Burruss and Laughrey, 2010, Fig. 5) may indicate interaction between water and gas precursors. Further research on organic matter conversion at high maturity is necessary to understand the details of secondary gas formation, and to improve interpretation of other phenomenon at high maturity such as variation of hydrogen isotopic composition of alkanes and the carbon isotopic composition of CO_2.

4.2. Geochemical significance

4.2.1. A complete trend of $\delta^{13}C$ versus maturity

The above results indicate that $\delta^{13}C$ values of gas from a single source rock do not necessarily increase linearly with maturity. We summarize the variation in Fig. 7. At lower maturity, with little or no contribution of secondary gas, there is a normal $\delta^{13}C$ trend with respects to carbon number and maturity trend (Region I). As maturity increases, the contribution of secondary gas becomes critical, and therefore $\delta^{13}C_2$ values become more negative with respect to maturity trend (Region II). The Barnett shale gas at high maturity falls in this range. As the maturity continues to increase, a reversal with respect to carbon number ($\delta^{13}C_2 < \delta^{13}C_1$) occurs (Region III), which is common in the eastern Sichuan Basin (Dai et al., 2004) and in the Western Canada Sedimentary Basin (Tilley et al., 2011). But at an even higher maturity, either due to decreased secondary gas contribution or its enrichment in ^{13}C, the trend may become normal again (Region IV). An example is the Weiyuan Gasfield in the Sichuan Basin ($\delta^{13}C_2$ and $\delta^{13}C_1$ range from −30 to −33‰ with $\delta^{13}C_2 > \delta^{13}C_1$ for most samples; Zhu et al., 2006) and the Kela-2 Gas Field in the Tarim Basin ($\delta^{13}C_2$ and $\delta^{13}C_1$ range from −16.6 to −19.4‰ and −26.2 to −28.2‰, respectively; Zhao et al., 2005).
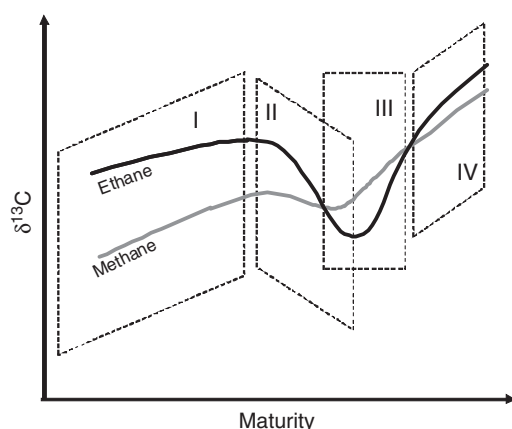
Fig. 7. A complete trend of maturity-dependent $\delta^{13}C_2$ and $\delta^{13}C_1$ variation. Regions: I — normal trend; II — $\delta^{13}C_2$ reversal with respect to maturity trend; III — $\delta^{13}C$ reversal against carbon number ($\delta^{13}C_1 > \delta^{13}C_2$); IV — normal trend.

The above analysis improves the understanding of gas-to-source-rock correlation for Paleozoic reservoirs in the Ordos Basin. From the hydrocarbon potential evaluation and exploration results, it has been confirmed that Permo-Carboniferous coal measures are the main source rock for the reservoirs in the Permo-Carboniferous terrigenous sandstone interlayers and in the underlying Ordovician weathered crust beneath the Ordovician/Carboniferous unconformity. Organic-poor Ordovician carbonate (measured TOC<0.2%) has little contribution (Xia, 2002). However, the $\delta^{13}C_2$ values of many gas samples from the Ordovician weathered crust are much more negative than those generated from Type III kerogen (Dai and Qi, 1989). This ethane has been explained as originating from another source rock containing sapropelic kerogen, such as Carboniferous carbonates. However, abundant Carboniferous sapropelic kerogen has not been discovered in the basin, so this explanation is questionable. In this work, the results of Fig. 5C and D and the mechanism of Fig. 7 provide an alternative interpretation: the ^{12}C rich ethane was generated from coal measures, but also has a contribution from secondary gas generation.

4.2.2. Conditions for the complete trend

The $\delta^{13}C$ reversal with respect to maturity trend was not commonly encountered in many previous natural gas isotope geochemistry studies, indicating some unique preconditions for its occurrence. A complete "normal and reversal" trend requires a wide range of source rock maturity. This condition may be satisfied by either a large basin area or a thick source rock interval, where R_o values vary continuously from less than 1.5% to over 2%. If the lower maturity range is absent, then only the "reversal" rangeappears, for example the conventional Carboniferous gas reservoirs in the eastern Sichuan Basin, China (Dai et al., 2004).

Additionally, stable tectonics and lithologic traps, including short migration distances, favor the reversed isotope trend. Source rock organic type or occurrence in a conventional or unconventional reservoirs(as shale gas) are not critical factors.

5. Conclusions

This study mainly demonstrates that mixing of primary and secondary gas in source rock can bring about alkane isotopic reversals versus carbon number and maturity. This mechanism probably accounts for the special phenomenon found in shale gas, where $\delta^{13}C_2$ first increases then becomes more negative with decreasing gas wetness. This mechanism indicates that reversed isotopic trends could be quite common, provided that the reservoir gas originated from one source rock having a large maturity variation and short migration distance. Entrapment of the gas within the source rock (shale gas) is not a requirement, because a similar phenomenon was also found in some conventional reservoirs. The precursor of the secondary gas is likely condensate retained in the source rock, which can contribute up to 30% of the total gas at high maturity.

References

Brown, D., 2010. Research getting unconventional boost. American Association of Petroleum Geologists Explorer 31, 8–10.
Burruss, R.C., Laughrey, C.D., 2010. Carbon and hydrogen isotopic reversals in deep basin gas: evidence for limits to the stability of hydrocarbons. Organic Geochemistry 41, 1285–1296.
Burruss, R.C., Ryder, R.T., 2003. Composition of crude oil and natural gas produced from 14 wells in the Lower Silurian "Clinton" sandstone and Medina Group, northeastern Ohio and northwestern Pennsylvania. U.S. Geological Survey Open File Report 03–409. 64 pp.

Dai, J., Qi, H., 1989. The $\delta^{13}C$–R_o relation of coal-formed hydrocarbon gas in China. Chinese Science Bulletin (Kexue Tongbao) 34, 690–692 (in Chinese).

Dai, J., Xia, X., Qin, S., Zhao, J., 2004. Origins of partially reversed alkane $\delta^{13}C$ values for biogenic gases in China. Organic Geochemistry 35, 405–411.

Dai, J., Li, J., Luo, X., Zhang, W., Hu, G., Ma, C., Guo, J., Ge, G., 2005. Stable carbon isotope compositions and source rock geochemistry of the giant gas accumulations in the Ordos Basin, China. Organic Geochemistry 36, 1617–1635.

Hill, R.J., Jarvie, D.M., Zumberge, J., Henry, M., Pollastro, R.M., 2007. Oil and gas geochemistry and petroleum systems of the Fort Worth Basin. American Association of Petroleum Geologists Bulletin 91, 445–473.

Hu, A.P., Li, J., Zhang, W.J., Li, Z.F., Hou, L., Liu, Q.Y., 2008. Geochemical characteristics and origin of gases from the Upper, Lower Paleozoic and the Mesozoic reservoirs in the Ordos Basin, China. Science in China, Series D: Earth Sciences 51 (zk1), 183–194.

Jenden, P.D., Drazan, D.J., 1993. Mixing of thermogenic natural gases in Northern Appalachian Basin. American Association of Petroleum Geologists Bulletin 77, 980–998.

Mullen, J., Lowry, J.C., 2010. Lessons learned developing the Eagle Ford Shale. Society of Petroleum Engineers Paper 138446-MS.

Passey, Q.R., Bohacs, K.M., Esch, W.L., Klimentidis, R., Sinha, S., 2010. From oil-prone source rock to gas-producing shale reservoir - geologic and petrophysical characterization of unconventional shale gas reservoirs. Society of Petroleum Engineers Paper 131350-MS.

Repetski, J.E., Ryder, R.T., Weary, D.J., Harris, A.G., Trippi, M.H., 2008. Thermal maturity patterns (CAI and %R_o) in upper Ordovician and Devonian rocks of the Appalachian Basin: a major revision of USGS Map I-917-E using new subsurface collections. U.S. Geological Survey Scientific Investigations Map 3006. 30 pp.

Rice, D.D., 1993. Composition and origins of coalbed gas. In: Law, B.E., Rice, D.D. (Eds.), Hydrocarbons from Coal: AAPG Studies in Geology, 38, pp. 159–184.

Rice, D.D., Clayton, J.L., Pawlewicz, M.J., 1989. Characterization of coal-derived hydrocarbons and source-rock potential of coal beds, San Juan Basin, New Mexico and Colorado, U.S.A. International Journal of Coal Geology 13, 597–626.

Schoell, M., 1983. Modeling thermogenic gas generation using carbon isotope ratios of natural gas hydrocarbons. American Association of Petroleum Geologists Bulletin 67, 2225–2238.

Stahl, W.J., Carey Jr., B.D., 1975. Source-rock identification by isotope analyses of natural gases from fields in the Val Verde and Delaware basins, West Texas. Chemical Geology 16, 257–267.

Stahl, W.J., Wollanke, G., Boigk, H., 1977. Carbon and nitrogen isotope data of Upper Carboniferous and Rotliegend natural gases from North Germany and their

relationship to the maturity of the organic source material. In: Campos, R., Gonji, J. (Eds.), Advances in Organic Geochemistry, pp. 539–559.

Tang, Y., Perry, J.K., Jenden, P.D., Schoell, M., 2000. Mathematical modeling of stable carbon isotope ratios in natural gases. Geochimica et Cosmochimica Acta 64, 2673–2687.

Tian, H., Xiao, X., Wilkins, R.W.T., Gan, H., Guo, L., Yang, L., 2010. Genetic origins of marine gases in the Tazhong area of the Tarim Basin, NW China: Implications from the pyrolysis of marine kerogens and crude oil. International Journal of Coal Geology 82, 17–26.

Tilley, B., McLellan, S., Hiebert, S., Quartero, B., Veilleux, B., Muehlenbachs, K., 2011. Gas isotope reversals in fractured gas reservoirs of the western Canadian Foothills: Mature shale gases in disguise. American Association of Petroleum Geologists Bulletin 95, 1399–1422.

Xia, X., 2000. Hydrocarbon Potential of Carbonates and Source Rock Correlation of the Changqing Gas Field. 1–164 pp. Petroleum Industry Press, Beijing. (in Chinese).

Xia, X., 2002. Rules of petroleum source correlation and their application in the Changqing gas field. Petroleum Exploration and Development 29, 101–105 (in Chinese with English abstract).

Xia, X., Tang, Y., 2012. Isotope fractionation of methane during natural gas flow with coupled diffusion and adsorption/desorption. Geochimica et Cosmochimica Acta 77, 489–503.

Xia, X., Zhao, L., Zhang, W., Li, J., 1999. Geochemical characteristics and source rock of Ordovician gas reservoir, Changqing Gasfield. Chinese Science Bulletin 44, 1917–1920.

Zhang, W., Li, J., 2001. Research on the oil and gas origin in the Ordos Basin. China Petroleum Exploration 6, 28–36 (in Chinese with English abstract).

Zhao, W., Zhang, S., Wang, F., Cramer, F., Chen, J., Sun, Y., Zhang, B., Zhao, M., 2005. Gas systems in the Kuche Depression of the Tarim Basin: Source rock distributions, generation kinetics and gas accumulation history. Organic Geochemistry 36, 1583–1601.

Zhu, G.Y., Zhang, S.C., Liang, Y.B., Ma, Y.S., Dai, J.X., Li, J., Zhou, G.Y., 2006. The characteristics of natural gas in Sichuan Basin and its sources. Earth Science Frontiers 13, 234–248 (in Chinese with English abstract).

Zumberge, J.E., Ferworn, K.A., Curtis, J.B., 2009. Gas character anomalies found in highly productive shale gas wells. Geochimica et Cosmochimica Acta 73, A1539.

Zumberge, J., Ferworn, K., Brown, S., 2012. Isotopic reversal ('rollover') in shale gases produced from the Mississippian Barnett and Fayetteville formations. Marine and Petroleum Geology 31, 43–52.